The Effect of Nonwoven Electrospun PAN Nanofiber Mat on Mechanical and Thermal Properties of Epoxy Composites

Mehmet Okan ERDAL[1], Şakir YAZMAN[2], Lokman GEMİ[*1], Ahmet YAPICI[3]

[1]Necmettin Erbakan University, Meram Vocational School, 42090, Konya
[2]Selcuk University, Ilgın Vocational School, 42600, Konya
[3]Iskenderun Technical University, Eng. & Natural Sciences Faculty, Mechanical Engineering Dep., 31200, Hatay

Abstract: In this study mechanical and thermal properties of epoxy resin reinforced with different numbers of nanofiber layers which produced with electrospinning method was investigated. Solution of 10 wt% of polyacrylonitrile (PAN) in N,N-dimethylformamide (DMF) was used for electrospinning. The diameters of the obtained nanofibers were in the range of 380-420 nm. The average thickness of the produced nanofiber layer was about 200 μm. The special molds were prepared to produce the laminated composite plates. The tensile tests show that the using of nanofiber PAN layers increase the tensile force 34.54% and decrease the elongation 8.87% in comparison with neat epoxy. The fracture surfaces of the specimens were inspected by using optical and scanning electron microscopy (SEM). The thermal properties of the nanofiber layered composites were determined by thermo gravimetric analysis (TGA) and differential scanning calorimetry (DSC) analysis. It was observed that the glass transition temperature increased parallel to this as the number of PAN layers increased and rose up to 86°C, while the thermal stability did not show much effect of PAN layers.

Örgülü Olmayan Elektrospin PAN Nanofiber Malzemenin Epoksi Kompozitlerin Mekanik ve Termal Özelliklerine Etkisi

Özet: Bu çalışmada elektrospin metodu ile üretilmiş farklı sayılardaki nanofiber takviyeli tabakalı epoksi kompozitlerin mekanik ve termal özellikleri araştırılmıştır. Elektrospin işlemi için ağırlıkça %10 oranında poliakrilonitril (PAN) ve N,N dimetilformamid (DMF) çözeltisi kullanılmıştır. Elde edilen nanofiber çapları 380-420 nm aralığındadır. Üretilen nanofiber tabaka kalınlığı ortalama 200 μm'dir. Tabakalı kompozit plakaları elde etmek için özel kalıplar hazırlanmıştır. Çekme deney sonuçları nanofiber tabaka kullanımının çekme kuvvetini saf epoksiye oranla % 34.54 arttırdığı ancak uzamayı saf epoksiye oranla % 8.87 azalttığı belirlenmiştir. Numunelerin kırılma yüzeyleri optik ve taramalı elektron mikroskopu (SEM) ile incelenmiştir. Üretilen nanofiber tabakalı kompozitlerin termal özellikleri termal gravimetrik analiz (TGA) ve diferansiyel taramalı kalorimetre (DSC) analizleri ile belirlenmiştir. Camsı geçiş sıcaklığının PAN tabaka sayısı arttıkça buna paralel olarak arttığı ve 86 °C ye kadar çıktığı, termal kararlılıkta ise PAN tabakalarının etkisinin çok fazla olmadığı görülmüştür.

1. Introduction

The epoxy resins are generally used as a matrix in composites materials and for their adhesive, chemical resistance, electrical insulation, low density and strong bond properties [1–3]. For achieving required mechanical and thermal properties, the approach of adding micro or nanofillers to polymer materials was applied [4,5]. The fibers which have diameters in nanometers show many good properties such as flexibility, large surface area and high mechanical performance [6].

The nanofiber reinforced composite laminates are expected to have an improved strength, interlaminar fracture toughness, and delamination resistance towards static, impact and fatigue loadings. Especially, the nanofibrous reinforcement could be useful to prevent delamination from any source such as matrix cracks, notches, holes, bolted joints, etc. The

aim of nanofibers is to bond adjacent plies and to reduce the stress concentration without reduction of in-plane properties. The matrix between adjacent plies of the laminate can be reinforced with nanofibers [7,8]. There are several techniques to produce the nanofibers like jet blowing, melt blowing, co-extrusion, interfacial polymerization, electrospinning and others [9–14]. The electrospinning method has been widely used, among these techniques, to produce nanofibers of polymer and to produce also nanofibers filled with various nanoparticles [15–22].

Many researches have been carried out on the use of nanofibers in laminated composites to enhance the mechanical performance. But, there are a few papers in the literature [23–27] and additional researches are required to be carried out on the benefits of electrospun nanofibers in composite materials.

This study presents an investigation of the use of polymeric nanofibrous layers to increase mechanical performance of the composite materials. The electrospun nanofibers of PAN layers are produced by electrospinning and placed in an epoxy. Three different layers were used to reinforce the epoxy. The fracture surface characterization is performed after the tensile test and the fiber breakage are investigated by using scanning electron microscopy (SEM).

2. Materials and Methods

2.1. Polymeric nanofibrous mats

Polyacrylonitrile (PAN) and pure N,N-dimethylformamide (DMF) were provided from Sigma–Aldrich. PAN granules were dissolved at 10 wt% in DMF. PAN solution was stirred at room temperature and stirred with magnetic stirrer to ensure its dissolution. A horizontal setup was used for electrospinning processes. A syringe was used as injector. The electrospinning setup consisted of a high voltage power supply, a syringe pump, a syringe and a grounded electrode connected with rotating drum.

The parameters for electrospinning processes were chosen as 20 kV voltage, the distance between the collector and the tip of the spinneret 15 cm and the feed rate 2 mL/h. The electrospinning setup is shown in Figure 1. The nanofibers were collected on a rotating drum. The fiber diameter and its alignment mainly depend on the applied voltage, flow rate and distance between needle and collector [28].

2.2. Thermal properties

The curing behavior of the neat epoxy, 1, 2 and 3 layer reinforced epoxy is investigated using DSC (METTLERTOLEDO DSC 1 STAR System) in a temperature range 20-350 °C. The thermal decomposition behavior of the composite specimens was carried out using TGA (METTLERTOLEDO TGA/DSC 2 STAR System) in the range 30– 800 °C.
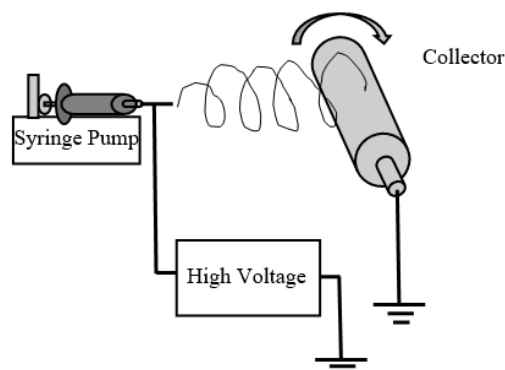

Figure 1. Electrospinning setup

2.3. FTIR

Fourier transform infrared (FTIR) spectrum measurements were performed by means of a BRUKER-Vertex 70 spectrophotometer. All analyses were made in the range between 400 and 4000 cm^{-1} with a resolution of 2 cm^{-1} at room temperature.

2.4. Specimen fabrication

The composite laminate production is summarized in Figure 2. In composite materials Momentive MGS L285 (diglycidyl ether of bisphenol A) was used as a resin and Momentive MGS H285 was used as a hardener. The PAN nanofibrous layers were placed in a special prepared mold then epoxy resin added. The mold is left for 24 hours at room temperature before it is placed into the oven for 80 °C temperature post cure for 15 hours.
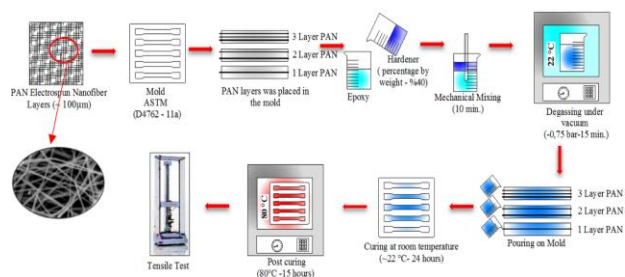

Figure 2. The fabrication scheme used to create the structure [29, 30]

Tensile testing of the composite specimens was carried out according to ASTM D638 on a Shimadzu model 10 kN universal testing machine. The experimental studies were repeated five times for each parameter.

3. Results and Discussion

3.1. Characterization of nanofibers

The morphology and structure of the PAN nanofibers were analyzed by SEM. Electrospun non-woven mats

were found to be 200 ± 10 μm thick and kept at room temperature for 24 h. The SEM image of electrospun fabric is shown in Figure 3. Fibers diameter (400 ± 20 nm) was measured by using image acquisition software.
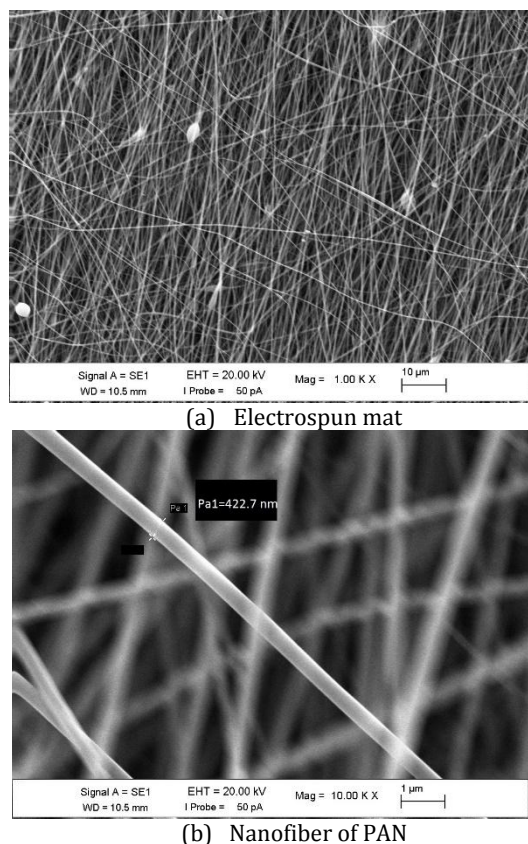

(a) Electrospun mat

(b) Nanofiber of PAN

Figure 3. Morphology of electrospun PAN fibers

3.2. DSC and TGA studies on the composites

As shown in Figure 4(a), DSC was used to analyze the neat epoxy and three different PAN layers/epoxy composites. The glass transition heat of epoxy resin T_g shows an endothermic peak at 64.33 °C. The glass transition temperature (T_g), reaction enthalpy (ΔH) and heat capacity (C_p) temperature for each composite are shown in Table 1. Figure 4(b) shows TGA results of neat epoxy and reinforced epoxy with various layers of PAN. The higher mass loss rate occurs at temperatures between 297 °C and 309 °C.

Table 1. The glass transition temperature (T_g), reaction enthalpy (ΔH) and heat capacity (C_p) temperature of samples.

Specimens	T_g (°C)	ΔH(j/g)	C_p (j/g°K)
Neat Epoxy	64	382	0.278
1 Layer PAN	80	285	0.142
2 Layer PAN	75	294	0.246
3 Layer PAN	86	290	0.201

The thermal parameters like T_{d5}- the initial decomposition temperature (the temperature of 5% weight loss), T_{onset}- the temperature at which the degradation started, T_d-degradation temperature and T_{endset}- the temperature at ending process were determined by the TGA as shown in Table 2.
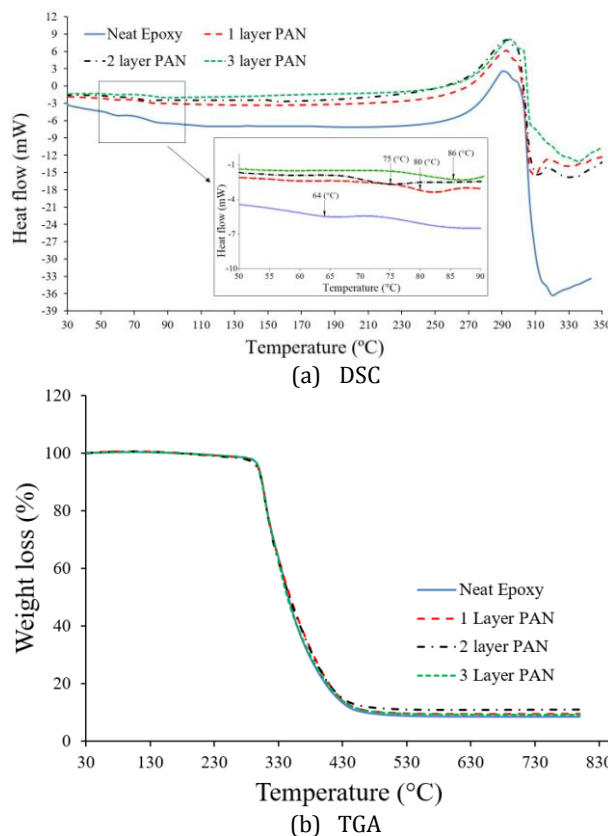

(a) DSC

(b) TGA

Figure 4. Thermograms of the specimens

Table 2. TGA parameters of samples obtained from TGA thermograms

Specimens	T_{onset} (°C)	T_{endset} (°C)	T_{d5} (°C)	T_d (°C)	Char (%) at 800°C
Neat Epoxy	175	628	299	306	8.5
1 Layer PAN	180	610	298	307	9.6
2 Layer PAN	170	584	297	308	10.9
3 Layer PAN	180	630	299	309	9.3

The results show that T_g values increase with the increasing of PAN layers compared to neat epoxy. The PAN layers show the catalytic effect in epoxy, they reduce the free space between macromolecular structures in the interface of PAN-epoxy. They increase also the crosslink intensity and decrease the unsaturated bonds. Similarly, by increasing the PAN layers the values of ΔH and C_p decrease. This means that the PAN layers in the composite absorb heat and act as a heat sink in the structure [31,32]. C_p generally related with the molecular mobility, the increase in molecular mobility gives higher ΔC_p values. Eventually increasing in T_g values cause decreasing in molecular mobility and C_p values.

Figure 4. and Table 1-2 show that there is no remarkable effect on thermal stability of epoxy with increasing the PAN layers.

3.3. FTIR spectra

The FTIR spectrum of nanofiber layers of PAN reinforced resin are depicted in Figure 5. and FTIR results for pure resin is given also for comparison. FTIR spectra of the resin with PAN layers prepared

was used to clarify the possible interaction between the epoxy resin and PAN layers. In the FTIR spectrum of the resin with PAN layers and without layers the characteristic absorption of the nanofibers based PAN layers was superposed over the pure epoxy resin structure.
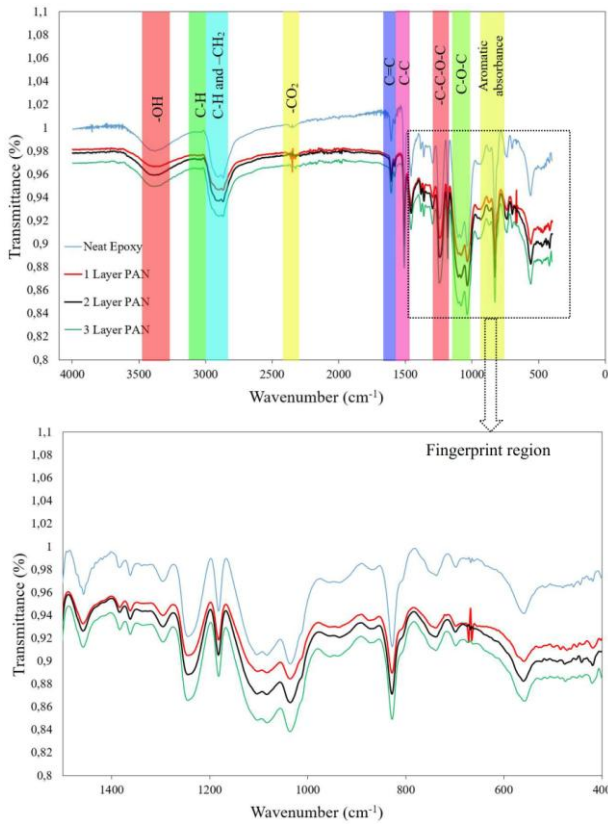

Figure 5. FTIR spectra of neat epoxy and nanofiber PAN layers

Chemical structure of epoxy resin based on bisphenol A, amino curing agent and PAN are given in Figure 6. Stretching vibration of different chemical groups of the neat epoxy and nanofiber PAN layers are given in Table 3 [33,34].

Two characteristic peaks at 2239 and 1447 cm^{-1} attributed to the $-C\equiv N$ stretching vibration and $-CH_2$ scissoring vibration of PAN polymer structure are not observed. No shifts can be detected in the fundamental vibration frequencies resulting from composite formation. Furthermore, the spectrum of nanofibers based PAN did not show any appearance or disappearance of bond formation between resin and PAN layers, which indicates that no new chemical bonds are formed in the interaction.

This situation supports the possible intermolecular interactions such as hydrogen binding, van der walls attractions and weak or strong dipol-dipol interactions between resin and PAN materials.

3.4. Tensile properties

The typical load-displacement diagram of the pure epoxy and three nanocomposites with the reinforcement content of one, two and three-layered plates are illustrated in Figure 7. The presented results show obvious changes in the mechanical behavior of the epoxy under tensile loading. The curves of reinforced epoxy show increasing of the value of load with a decrease in the plastic region comparing to the neat epoxy (Figure 8 (a-d)).
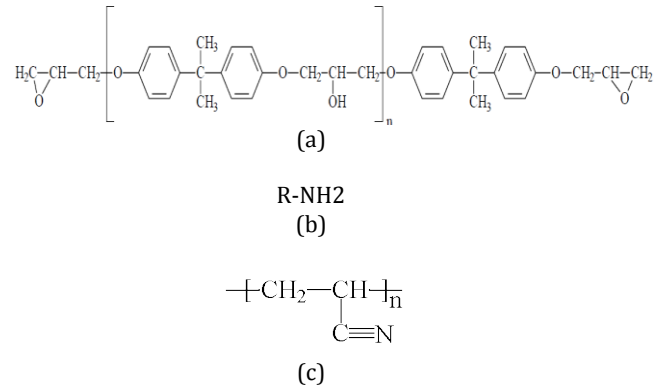

Figure 6. Chemical structure of a) epoxy resin based on bisphenol A, b) amino curing agent and c) PAN

Table 3. Stretching vibration of different chemical groups of the neat epoxy and nanofiber PAN layers

Bands (cm^{-1})	Assignment
3340-3500	Hydroxyl (–OH) stretching
3060	Symmetric stretching of C–H of the oxirane ring
2960-2870	Alkyl units (C–H and –CH2) stretching
2349	$-CO_2$
1607	C=C stretching of aromatic ring
1509	C–C stretching of aromatic ring
1236	–C–C–O–C stretching
1036	C–O–C stretching of ethers
828	Aromatic absorbance

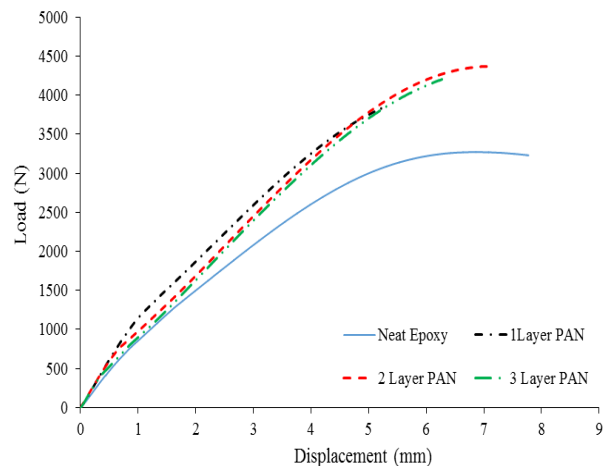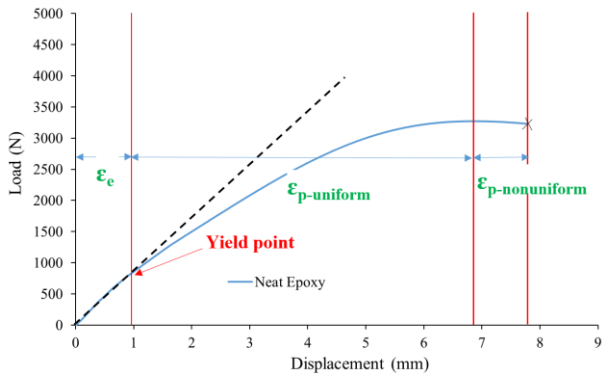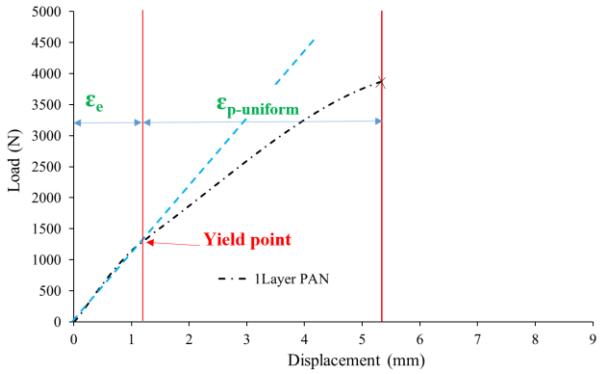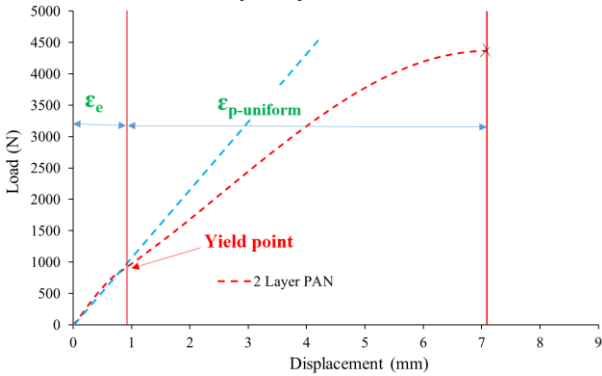**Figure 7.** Tensile graphs of the composites with different layer numbers

The tensile test results of epoxy and composites are given in Figure 9. The highest improvements of these four graphs were achieved for two-layered PAN composite with enhancement of 34.54% in tensile strength while elongation decreases 8.87% compared with neat epoxy.
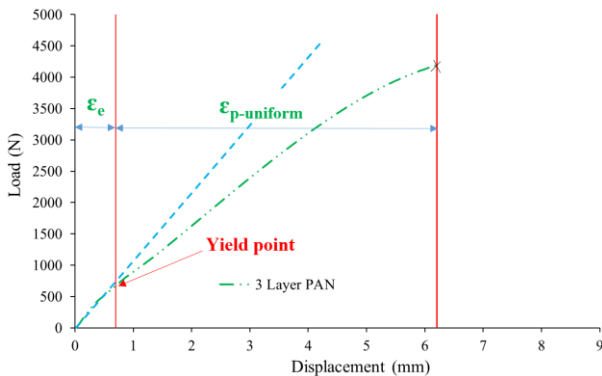
a) Neat epoxy

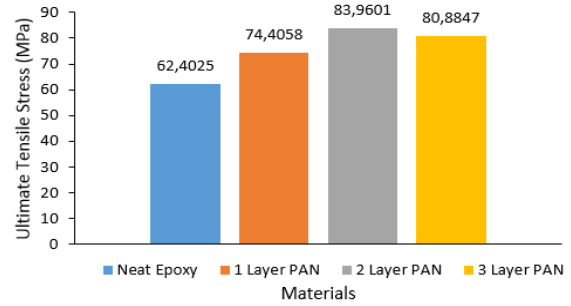

b) 1 Layer PAN

c) 2 Layer PAN

d) 3 Layer PAN

Figure 8. The yield points and plastic deformation regions of neat epoxy and composites in the tensile graphs.
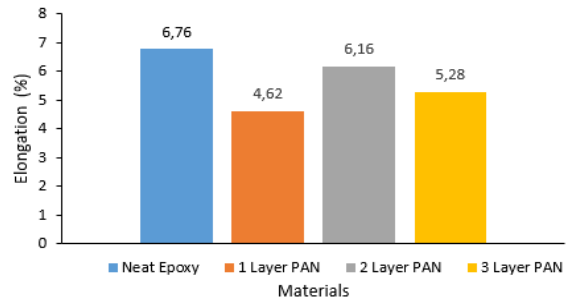
3.5. Structural and morphological characterization after tensile tests

Figure 10. shows cross-sectioning and optical microscope study after tensile tests. The Figures

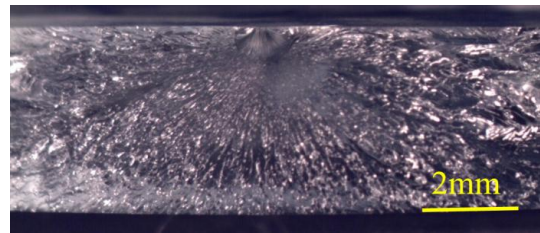10(b-d) show that PAN layers are straight, tight and bonded perfectly with epoxy.
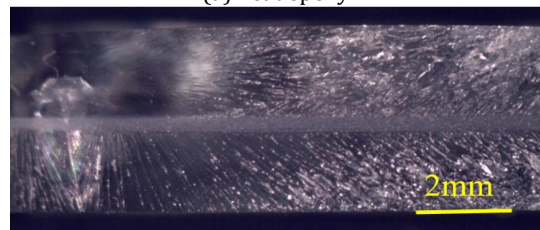

(a) Ultimate tensile stress
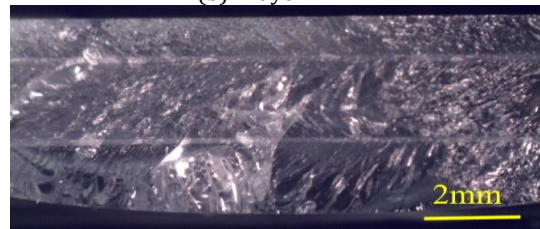

(b) Elongation at break (%)

Figure 9. Tensile tests results
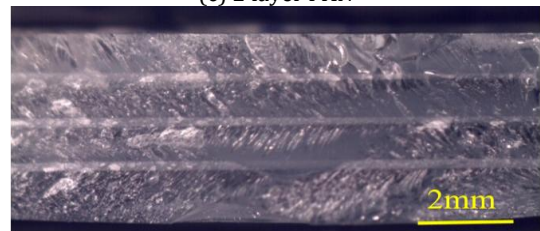

(a) neat epoxy

(b) 1 layer PAN

(c) 2 layer PAN

(d) 3 layer PAN

Figure 10. Optical microscopy

SEM fractographs were taken after failure of the specimens at various points. The matrix cracks inclined towards the direction of crack propagation Figure 11(a-b).
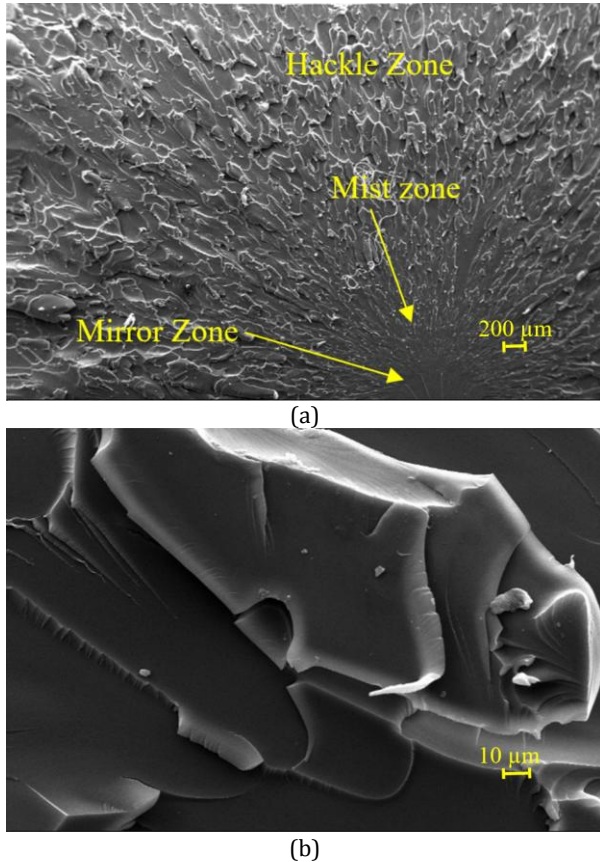

(a)

(b)

Figure 11. SEM pictures of fractured surfaces of neat epoxy (a) X21 (b) X500 magnification.

Figure 12. shows the detailed PAN-epoxy bond and crack propagation lines on cross-sectioning surface of the specimen. It is obvious that the PAN layer bonded perfectly with epoxy. Generally, mirror, mist and hackle three different fracture zones observed in case of thermosetting polymers [35]. The three fracture zones can be seen on the fracture surface of neat epoxy and PAN reinforced epoxy as shown in Figure 11(a) and Figure 12(a). The crack propagation direction is indicated by red color arrows. At the beginning of the fracture the crack grows very slowly and creates very smooth surface (mirror zone) [36,37]. Then the crack accelerates and creates a little rougher region (mist zone). When the crack reaches its maximum speed a very rough region occurs (hackle zone). Investigating Figure 12(a), crack propagates in PAN layer faster than in epoxy from left to right and creates mirror zone (about ± 45° crack lines) around the PAN layer. This result is compatible with the result of tensile test. Because the catalytic effect in the interface of PAN- epoxy increases the crosslink intensity and decreases the unsaturated bonds making the composite plate brittle than neat epoxy and increasing the strength (Figure 7). Figure 12(d) shows also the debonding and pullout of the nanofiber of PAN from epoxy and nanofiber breakage after tensile test [38,39].
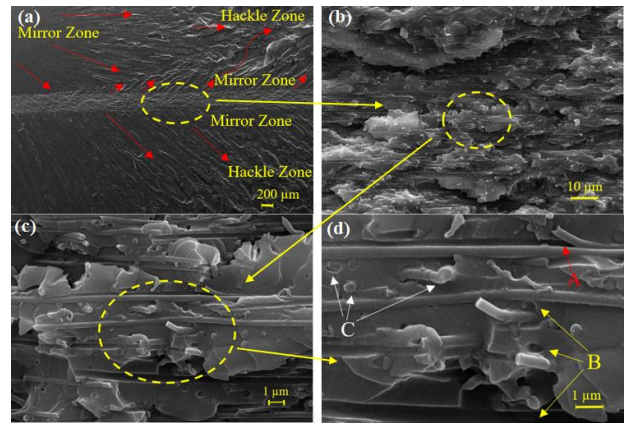

Figure 12. SEM images of tensile fracture surface of 1 layer PAN-epoxy (a) X20 (b) X1000 (c) X5000 (d) X10000 magnification; where A-debonding, B-pullout, C-breakage.

4. Conclusions

The nanofiber PAN layers were produced using electrospinning by dissolving PAN in DMF solution. PAN layers are placed in epoxy using special mold. Thermal and mechanical properties of neat epoxy, one-layer PAN, two-layer PAN and three-layer PAN reinforced composites plates were investigated.

DSC results show that the PAN layers/epoxy composites have slight higher temperature range comparing to neat epoxy. TGA thermograms show that there is no remarkable effect on thermal stability of epoxy with increasing the PAN layers. As a result of tensile tests, PAN layers increase the tensile stress but they decrease the elongation. Two-layered composite gives the highest tensile load value.

References

[1] Ueki, T., Nishijima, S., Izumi, Y. 2005. Designing of epoxy resin systems for cryogenic use. Cryogenics, 45(2), 141–8.

[2] Kang, S., Hong, SI., Choe, CR., Park, M., Rim, S., Kim, J. 2001. Preparation and characterization of epoxy composites filled with functionalized nanosilica particles obtained via sol–gel process. Polymer, 42(3), 879–87.

[3] Shan, X., Huang, C., Yang, H., Wu, Z., Li, J., Huang, R., et al. 2015. The thermal expansion and tensile properties of nanofiber-ZrW2O8 reinforced epoxy resin nanocomposites. Phys Procedia, 67, 1056–61.

[4] Chen, IH., Wang, CC., Chen, CY. 2010. Preparation of carbon nanotube (CNT) composites by

polymer functionalized CNT under plasma treatment. Plasma Process Polymers, 7(1), 59–63.

[5] Li, J., Wu, Z., Huang, C., Liu, H., Huang, R., Li, L. 2014. Mechanical properties of cyanate ester/epoxy nanocomposites modified with plasma functionalized MWCNTs. Composites Science and Technology, 90,166–73.

[6] Huang, ZM., Zhang, YZ., Kotaki, M., Ramakrishna, S. 2003. A review on polymer nanofibers by electrospinning and their applications in nanocomposites. Composites Science and Technology, 63(15), 2223–53.

[7] Palazzetti, R., Zucchelli, A., Gualandi, C., Focarete, ML., Donati, L., Minak, G., et al. 2012. Influence of electrospun Nylon 6,6 nanofibrous mats on the interlaminar properties of Gr-epoxy composite laminates. Composite structures, 94(2), 571–9.

[8] Kim, JS., Reneker, DH. 1999. Mechanical properties of composites using ultrafine electrospun fibers. Polymer Composites, 20(1), 124–31.

[9] Borkar, S., Gu, B., Dirmyer, M., Delicado, R., Sen, A., Jackson, BR., et al. 2006. Polytetrafluoroethylene nano/microfibers by jet blowing. Polymer, 47(25), 8337–43.

[10] Ellison, C.J, Phatak, A., Giles, DW., Macosko, CW., Bates, FS. 2007. Melt blown nanofibers: Fiber diameter distributions and onset of fiber breakup. Polymer, 48(11), 3306–16.

[11] Wang, J., Langhe, D., Ponting, M., Wnek, GE., Korley, LT., Baer, E. 2014. Manufacturing of polymer continuous nanofibers using a novel co-extrusion and multiplication technique. Polymer, 55(2), 673–85.

[12] Zhang, X., Zhu, J., Haldolaarachchige, N., Ryu, J., Young, D. P., Wei, S., Guo, Z. 2012. Synthetic process engineered polyaniline nanostructures with tunable morphology and physical properties. Polymer, 53(10), 2109-2120.

[13] Zhao, S., Wu, X., Wang, L., & Huang, Y. 2004. Electrospinning of ethyl–cyanoethyl cellulose/tetrahydrofuran solutions. Journal of Applied Polymer Science, 91(1), 242-246.

[14] Yang, F., Murugan, R., Wang, S., Ramakrishna, S. 2005. Electrospinning of nano/micro scale poly (L-lactic acid) aligned fibers and their potential in neural tissue engineering. Biomaterials, 26(15), 2603-2610.

[15] Bhardwaj, N., Kundu, S. C. 2010. Electrospinning: A fascinating fiber fabrication technique. Biotechnology Advances, 28(3), 325-347.

[16] Jeun, JP., Kim, YK., Lim, YM., Choi, JH., Jung, CH KP., Yc, N. 2007. Electrospinning of Poly (L-lactide-co-D, L-lactide). Journal of Industrial and Engineering Chemistry, 13(4), 592-596.

[17] Demir, MM., Yilgor, I., Yilgor, E., Erman, B. 2002. Electrospinning of polyurethane fibers. Polymer, 43(11), 3303-3309.

[18] Zhu, J., Wei, S., Rutman, D., Haldolaarachchige, N., Young, DP., Guo, Z. 2011. Magnetic polyacrylonitrile-Fe@ FeO nanocomposite fibers-Electrospinning, stabilization and carbonization. Polymer, 52(13):2947–2955.

[19] Zhu, J., Chen, M., Qu, H., Wei, H., Guo, J., Luo, Z., Guo, Z. 2014. Positive and negative magnetoresistance phenomena observed in magnetic electrospun polyacrylonitrile-based carbon nanocomposite fibers. Journal of Materials Chemistry C, 2(4), 715-722.

[20] Tomczak, N., Gu, S., Han, M., van Hulst, NF., Vancso, G.J. 2006. Single light emitters in electrospun polymer nanofibers: Effect of local confinement on radiative decay. European polymer journal, 42(10), 2205-2210.

[21] Qu, H., Wei, S., Guo, Z. 2013. Coaxial electrospun nanostructures and their applications. Journal of Materials Chemistry A, 1(38), 11513-11528.

[22] Almuhamed, S., Khenoussi, N., Bonne, M., Schacher, L., Lebeau, B., Adolphe, D., Brendlé, J. 2014. Electrospinning of PAN nanofibers incorporating SBA-15-type ordered mesoporous silica particles. European polymer journal, 54, 71-78.

[23] Shivakumar, K., Lingaiah, S., Chen, H., Akangah, P., Swaminathan, G., Russell, L. 2009. Polymer nanofabric interleaved composite laminates. AIAA journal, 47(7), 1723-1729.

[24] Sihn, S., Kim, RY., Huh, W., Lee, KH., Roy, AK. 2008. Improvement of damage resistance in laminated composites with electrospun nano-interlayers. Composites Science and Technology, 68(3-4), 673-683.

[25] Liu, L., Huang, ZM., He, CL., Han, X. 2006. Mechanical performance of laminated composites incorporated with nanofibrous membranes. Materials Science and Engineering: A, 435, 309-317.

[26] Zhang, J., Lin, T., Wang, X. 2010. Electrospun nanofibre toughened carbon/epoxy composites: Effects of polyetherketone cardo (PEK-C) nanofibre diameter and interlayer thickness. Composites Science and Technology, 70(11), 1660-1666.

[27] Lin, S., Cai, Q., Ji, J., Sui, G., Yu, Y., Yang, X., Deng, X. 2008. Electrospun nanofiber reinforced and toughened composites through in situ nano-interface formation. Composites Science and Technology, 68(15-16), 3322-3329.

[28] Akangah, P., Lingaiah, S., Shivakumar, K. 2010. Effect of Nylon-66 nano-fiber interleaving on impact damage resistance of epoxy/carbon fiber composite laminates. Composite Structures,

92(6), 1432-1439.

[29] Erdal, MO., Yazman, Ş., Gemi, L., Yapıcı, A. 2015. Çok Katmanlı Nanoelyaf Takviyesinin Epoksi Reçinenin Mekanik Özelliklerine Etkisinin İncelenmesi. Mühendislikte Yeni Teknolojiler Sempozyumu, 22-23 Ekim, Bayburt, 30-35.

[30] Jin, F-L., Ma, C-J., Park, S-J. 2011. Thermal and mechanical interfacial properties of epoxy composites based on functionalized carbon nanotubes. Materials Science and Engineering: A, 528(29-30), 8517-8522.

[31] Yapici, A., Özkan, V., Yıldız, M., Erdal, M., Gemi, L., Yazman, Ş. 2016. The Effect of Nylon 6.6 Nanofiber Layers on Mechanical Properties of Epoxy. The International Journal of Engineering and Science, 5(11), 86-89.

[32] Yapici, A., Özkan, V., Yıldız, M., Erdal, M., Gemi, L., Yazman, Ş. 2016. The nylon 6.6 nanofiber layers' effect on mechanical properties of epoxy. 12th International Nanoscience and Nanotechnology Conference, 03-05 June Kocaeli, 152.

[33] Tait, J., Davies, G., McIntyre, R., Yarwood, J. 1997. FTIR-ATR studies of interfacial interactions in epoxy resin/polymer laminate structures. Vibrational spectroscopy, 15(1), 79-89.

[34] Nacimiento, F., Alcántara, R., González, JR., Tirado, JL. 2012. Electrodeposited polyacrylonitrile and cobalt-tin composite thin film on titanium substrate. Journal of The Electrochemical Society, 159(7), A1028-A1033.

[35] Goyat, M., Suresh, S., Bahl, S., Halder, S., & Ghosh, P. 2015. Thermomechanical response and toughening mechanisms of a carbon nano bead reinforced epoxy composite. Materials Chemistry and Physics, 166, 144-152.

[36] Gemi, L., Yazman, Ş., Uludağ, M., Dışpınar, D. 2017. The effect of 0.5 wt% additions of carbon nanotubes & ceramic nanoparticles on tensile properties of epoxy-matrix composites: A comparative study. Materials Science and Nanotechnology, 1(2), 15-22.

[37] Yazman, Ş., Gemi, L., Uludağ, M., Dışpınar, D. 2015. Investigation of The Effect of Carbon Nanotube Ratio on The Wear Behavior of Carbon Nanotube/Epoxy Nanocomposites. International Journal of Enhanced Research in Science, Technology & Engineering, 4(7), 201-207.

[38] Güneş, E., Erdal, M., Gemi, L. 2017. The effect of nanofiber on the biological traits of Drosophila Melanogaster. Sakarya University Journal of Science, 26(6), 1612-1617.

[39] Morkavuk, S., Köklü, U., Bağcı, M., Gemi, L. 2018. Cryogenic machining of carbon fiber reinforced plastic (CFRP) composites and the effects of cryogenic treatment on tensile properties: A comparative study. Composites Part B: Engineering, 147, 1-11.